

Enriched HLA-E and CD94/NKG2A interaction limits antitumor CD8⁺ tumor-infiltrating T lymphocyte responses

Megat Abd Hamid^{1,3,8}, Ruo-zheng Wang^{2,4,8}, Xuan Yao^{1,3,8}, Peiwen Fan^{2,4,8}, Xi Li^{1,3}, Xuemei Chang^{2,4}, Yaning Feng^{2,4}, Stephanie Jones⁵, David Maldonado-Perez^{5,6}, Craig Waugh⁷, Clare Verrill^{5,6}, Alison Simmons^{1,3}, Vincenzo Cerundolo^{1,3}, Andrew McMichael¹, Christopher Conlon¹, Xiyan Wang^{3,4}, Yanchun Peng^{1,2,3,8}, Tao Dong^{1,2,3,4,8,*}

¹CAMS-Oxford International Centre for Translational Immunology, CAMS Oxford Institute, Nuffield Department of Medicine, University of Oxford, Oxford, UK. ²Chinese Academy of Medical Sciences (CAMS) Key Laboratory of Tumor Immunology and Radiation Therapy, Third Affiliated Hospital, Xinjiang Tumor Hospital, Urumqi, China. ³MRC Human Immunology Unit, Weatherall Institute of Molecular Medicine, Radcliffe Department of Medicine, University of Oxford, Oxford, UK. ⁴Third Affiliated Hospital, Xinjiang Tumor Hospital, Urumqi, China. ⁵Oxford Radcliffe Biobank, Department of Cellular Pathology, Oxford University Hospitals NHS Trust, Oxford, UK. ⁶Oxford NIHR Biomedical Research Centre, Nuffield Department of Surgical Sciences, University of Oxford, Oxford, UK. ⁷Flow Cytometry Facility, Weatherall Institute of Molecular Medicine, University of Oxford, Oxford, UK. ⁸Authors contributed equally

*Correspondence(s): (1) Tao Dong, email address: tao.dong@imm.ox.ac.uk, telephone number: +441865222443. (2) Ruo-zheng Wang, email address: wrz8526@163.com

Running title: Enriched HLA-E and CD94/NKG2A impair CD8⁺ TILs responses

Conflict of Interest statement: The authors declare no potential conflicts of interest.

Funding support: Chinese Academy of Medical Sciences (CAMS) Innovation Fund for Medical Sciences (CIFMS), China (grant number: 2018-I2M-2-002 and 2017PT31043); Medical Research Council, United Kingdom (MR/L018942/1 and MRC Human Immunology Unit Core). MAH is funded by the Malaysia's King Scholarship, CV research time is supported by the National Institute of Health Research (NIHR) Oxford Biomedical Research Centre (BRC) (Molecular Diagnostics Theme/Multimodal Pathology Subtheme) and DMP is funded by the NIHR Oxford BRC (Molecular Diagnostics Theme/Multimodal Pathology Subtheme).

Abstract

Immunotherapy treatments with anti-PD-1 boost recovery in less than 30% of treated cancer patients, indicating the complexity of the tumor microenvironment. Expression of human leukocyte antigen-E (HLA-E) is linked to poor clinical outcomes in mice and human patients. However, the contributions to immune evasion of HLA-E, a ligand for the inhibitory CD94/NKG2A receptor, when expressed on tumors, compared to adjacent tissue and peripheral blood mononuclear cells, remains unclear. In this study, we report that epithelial-derived cancer cells, tumor macrophages, and CD141⁺ conventional dendritic cells (cDC) contributed to HLA-E enrichment in carcinomas. Different cancer types showed a similar pattern of enrichment. Enrichment correlated to NKG2A upregulation on CD8⁺ tumor-infiltrating T lymphocytes (TILs) but not on CD4⁺ TILs. CD94/NKG2A is exclusively expressed on PD-1^{high} TILs while lacking intratumoral CD103 expression. We also found that the presence of CD94/NKG2A on human tumor-specific T cells impairs IL2 receptor-dependent proliferation, which affects IFN γ -mediated responses and antitumor cytotoxicity. These functionalities recover following

antibody-mediated blockade *in vitro* and *ex vivo*. Our results suggest that enriched HLA-E:CD94/NKG2A inhibitory interaction can impair survival of PD-1^{high} TILs in the tumor microenvironment.

Keywords

Human leukocyte antigen-E; inhibitory CD94/NKG2A; TILs

Introduction

Avoidance of immune destruction is a hallmark of cancer. Tumor employs diverse mechanisms to escape antitumor immunity such as by enhancing the immune checkpoint expression of PD-1 on TILs and by downregulating the MHC-Ia surface expression on cancer cells (1-3). These changes reduce the efficacy of tumor-localized T cell priming, leading to impaired antitumor immunity and increased tumor progression. Although past clinical studies of checkpoint blockade using anti-PD-1 or anti-CTLA-4 have shown improvement in some patients, these treatments failed to improve overall response rates in many anti-PD-1 treated cancer patients (4-7).

Various studies have associated an enrichment of the non-classical MHC-Ib molecule, HLA-E, with poorer clinical outcome in cancer patients (8-13). For example, high numbers of head-and-neck cancer patients were found to have HLA-E enriched carcinomas, corresponding to lower survival rates as tumor progresses. On the other hand lymphoma-treated Qa-1^b knockout mice (Qa-1^b is the murine HLA-E homologue) have better tumor regression (12, 13). Nevertheless, whether HLA-E is enriched specifically in carcinoma compared to adjacent tissue or blood of patients and whether

this enrichment negatively affects antitumor T cell responses in humans remains unclear.

Although MHC-Ia molecules help in cancer cell recognition through the T cell receptor, HLA-E can be recognized by the inhibitory heterodimeric CD94/NKG2A ligand (14). This interaction inhibits NK cell cytotoxic functions and prevents autoimmunity but is also exploited by cytomegalovirus to evade anti-viral immunity (15-19). In a phase II human clinical trial, treatment of head and neck cancer patients with anti-NKG2A in combination with anti-EGFR demonstrated improvement in overall response rates in the majority of the patients (12). However, it is still unknown in other human cancers whether the HLA-E:CD94/NKG2A inhibitory machinery could also be exploited by cancer to impair TIL priming capacity and inhibit antitumor T cell responses.

The efficacy of T-cell priming in cancer relies on the uptake and presentation of neoantigen by antigen-presenting cells (APCs) via the MHC-Ia molecules. For example, tumor-localized CD141⁺ cDC enable prolonged tissue-localized cross-priming of T cell activation and maintenance (20, 21), whereas tumor-infiltrating macrophages treated with anti-CD47 showed improved phagocytosis and antigen priming capacity in murine model (22). However, studies using DC vaccines that solely targeted the recovery of MHC-Ia surface expression on tumor APC failed to improve outcomes in mice and cancer patients (23-25). This is thought to be due to the expression of inhibitory receptors such as PD-1 on tumor-localized APCs that affected the efficacy of MHC Ia–T cell priming and contributed to further tumor growth (26-28). It is therefore likely that an enriched inhibitory HLA-E presence in tumor could also interfere with efficient DC

presentation of tumor neoantigens by dampening and masking MHC class Ia–Tcell priming via the CD94/NKG2A interaction.

Thus, in this study, we sought to investigate with human tissues and cells the correlation between HLA-E and CD94/NKG2A expressions as well as the phenotype of CD94/NKG2A⁺ T cells from paired tumor, paratumor and PBMC samples of cancer patients. In addition, we investigated the potential of enriched HLA-E:CD94/NKG2A interaction to impair human antitumor T cell function. We found that HLA-E enrichment on carcinoma tissue derives from epithelial-derived cancer cells, tumor-localized DCs and macrophages. Effector CD8⁺ TILs but not regulatory CD4⁺ TILs have enriched CD94/NKG2A presence that is associated with PD-1^{high} expression but antagonistic to tissue resident CD103 marker expression. We found that the enriched presence and interaction of HLA-E with CD94/NKG2A significantly impairs IL2 receptor-dependent proliferation of tumor-specific T cells, that contributed to reduced cytotoxicity and cytokine production, which improved following antibody-mediated blockade treatment *in vitro* and *ex vivo*. Altogether, our work highlights the inhibitory role of enriched HLA-E and CD94/NKG2A on antitumor T cell functions and the overall exhaustive nature of TILs, which makes them a good target for human cancer immunotherapy in various gastrointestinal cancer types.

Materials and Methods

Study subjects

This study was approved by the Oxford Radcliffe Biobank (ORB) research ethics committee (reference number: 09/H0606/5+5) and the Ethics Committee of the Third

Affiliated Tumor Hospital of Xinjiang Medical University (reference number: K-201403), based on the guidelines of the Declaration of Helsinki. The average age of the patients was 58.18 years (range of 39 to 81 years). Similar sizes of tissues samples were collected from each patient. Samples were of adenocarcinoma without metastasis, with resection volume no less than 0.5*0.5*0.5cm. Tumor was confirmed using immunohistopathology. Written informed consent was obtained from all subjects prior to inclusion in the study. General stratification of patients is described in **Supplementary Table S1**.

Isolation of lymphocytes from paired blood and tissues

PBMC were isolated from fresh heparinized blood by Ficoll-Hypaque density gradient centrifugation. Mononuclear cells were isolated from tumor and paratumor tissues using Miltenyi tumor dissociation kit as commercially described. Lymphocytes were isolated using Ficoll-Hypaque density gradient centrifugation.

Generating antigen-specific T cell lines

Antigen-specific T cell lines were generated as previously described (29). Briefly, isolated lymphocytes from blood and tissues were stimulated with either cancer SSX2₄₁₋₄₉-specific KV9 peptide (KASEKIFYV) or CMV pp65₄₉₅₋₅₀₃-specific NV9 peptide (NLVPMVATV) and cultured in RPMI-1640 supplemented with 10% v/v heat-inactivated human AB serum (National Blood Service, UK), 2mM L-Glutamine and 1% v/v (500U/ml) penicillin streptomycin (Sigma-Aldrich, UK) and recombinant human IL2 (Peprotech, UK) at 37°C. After 14 days, antigen-specific T cells were purified with peptide-MHC Class I tetramer (HLA-A2 KV9 or HLA-A2 NV9) using BD Aria II (BD

Biosciences) and later expanded *in vitro*. The cell lines were confirmed for antigen-specificity using tetramer staining by flow cytometry and all functional assays were performed using peptide-specific stimulation.

Generation of HLA-E^{high} EBV-transformed B cell line (BCL)

An HLA-A2⁺ Epstein-Barr virus-transformed B cell line was generated in the lab at 2005 and maintained in RPMI-1640 supplemented with 10% v/v fetal calf serum (Sigma Aldrich), 2mM L-glutamine and 1% v/v (500 U/ml) penicillin streptomycin (Sigma-Aldrich, UK) at 37°C. Surface expression of CD19 and HLA-A2 on this BCL was assessed regularly by flow cytometry staining. Lentiviruses expressing either HLA-E0101 or HLA-E0103 allele were generated using the three plasmids system by co-transfection of 293T cell line cultured in DMEM supplemented with 10% v/v fetal calf serum (Sigma Aldrich), 2mM L-Glutamine and 1% v/v (500U/ml) penicillin streptomycin (Sigma-Aldrich, UK) at 37°C, as previously described (29). After 48hours, supernatant containing lentivirus was collected, filtered and later concentrated using Lenti-XTM Concentrator (ClonTech) according to manufacturer's instruction. The HLA-A2⁺ BCL was then transduced with either HLA-E0101 or HLA-E0103 lentivirus and cultured for 5 days at 37°C before sorted for HLA-E high expression using BD Aria II (BD Biosciences) and grown in complete media at 37°C. After 7 days, HLA-E expression was confirmed using flow cytometry, with wild-type HLA-A2⁺ BCL as negative control. All cell lines were tested for Mycoplasma monthly.

***Ex vivo* flow cytometry staining**

Cells isolated from tissues and PBMC were first stained with LIVE/DEAD® Fixable Aqua Dead Cell Stain Kit (ThermoFischer Scientific) then stained with conjugated antibodies, with incubation at each step for 20minutes at 4°C. Tetramer staining was performed as previously described (29). Briefly, cells were stained with either HLA-A2 KV9 or HLA-A2 NV9 tetramer for 20minutes at 37°C before continuing with abovementioned staining process. All samples were acquired on BD LSR Fortessa (BD Biosciences) flow cytometer and analyzed using FlowJo™ v.10 software (Tree Star Inc.).

Antibody specificities and coupled labels used for surface staining included: Alexa Flour488-MHC-1a (clone W6/32; BioRad; RRID:AB_322094), PE-HLA-E (3D12; Biolegend; RRID:AB_1659249), BV421-EpCAM (EBA-1; BD Biosciences; RRID:AB_2738050), PerCP/Cy5.5-CD163 (GHI/61; Biolegend; RRID:AB_2228986), BV650-αCD123 (6H6; Biolegend; RRID:AB_2563827), BV421-CD1c (L161; Biolegend; RRID:AB_10962909), BV605-CD141 (M80; Biolegend; RRID:2572199), BV711-CD14 (M5E2; Biolegend; RRID:AB_2562909), PE/Cy5-CD20 (2H7; Biolegend; RRID:AB_314256), BV785-HLA-DR (L243; Biolegend; RRID:AB_2563461), APC/Cy7-CD11b (ICRF44; Biolegend; RRID:AB_2563395), BV510-CD3 (OKT3; Biolegend; RRID:AB_2561943), BV510-CD16 (3G8; Biolegend; RRID:AB_2562085), BV510-CD56 (HCD56; Biolegend; RRID:AB_2561944), BV510-CD19 (HIB19; Biolegend; RRID:AB_2561668), BV510-CD141 (1A4; BD Biosciences; RRID:AB_27828103), BV510-CD14 (M5E2; Biolegend; RRID:AB_2561946), BV510-CD1c (L161; Biolegend; RRID:AB_2566119), BV510-CD163 (GHI/61; Biolegend; RRID:AB_2650632), BV510-CD123 (6H6; Biolegend; RRID:AB_2562068), BV785-CD3 (OKT3; Biolegend; RRID:AB_2563507), PerCP/Cy5.5-CD8 (SK1; BD Biosciences; RRID:AB_2687497),

APC/H7-CD4 (SK3; BD Biosciences; RRID:AB_1645732), PE-Texas Red- α CD56 (HCD56; Biolegend; RRID:AB_2563564), FITC-CD94 (HP-3D9; BD Biosciences; RRID:AB_396200), APC-NKG2A (131411; R&D Systems; RRID:AB_356987), PE/Cy7-CD27 (M-T271; Biolegend; RRID:AB_2562258), BV421-CCR7 (G043H7; Biolegend; RRID:AB_11203894), BV605-CD45RA (HI100; Biolegend; RRID:AB_2563814), PE-CD4 (SK3; BD Biosciences; RRID:AB_400079), BV650-PD-1 (EH12.2H7; Biolegend; RRID:AB_2566362), BV711-KLRG-1 (2F1/KLRG-1; Biolegend; RRID:AB_2629721), and APC-BTLA (MIH26; Biolegend; RRID:AB_10613101).

T cell proliferation assay

HLA-E^{high} BCL (generated as mentioned above) or commercially available HCT116 colorectal cancer cell line (CCL-247; ATCC) were stimulated *in vitro* with specific peptides at different concentrations. Ex vivo TILs were stimulated with 1 μ M *Staphylococcal enterotoxin B* (SEB; Sigma Aldrich) for one hour at 37°C. T cell lines were stained with 0.5 μ M CFSE before being co-cultured with peptide-stimulated HLA-E^{high} BCL or HCT116. After 30 hours, cells were stained for IL2 receptor expression (PE-anti-CD25 (M-A251; Biolegend; RRID:AB_2561861)). After 72 hours incubation, cells were measured for CFSE fluorescence. To evaluate the change in response, T cells were treated with either Ultra-LEAF purified mouse IgG1 kappa isotype Control (MG1-45; Biolegend; RRID:AB_11148942) or 15ug/ml purified anti-CD94 (DX22; Biolegend; RRID:AB_314532) plus 5ug/ml purified anti-NKG2A (Z199; Beckman Coulter; RRID:AB_131495) for 15 minutes at 37°C before the co-culture.

Cytokine production assessment

For *in vitro* cytokine production, supernatant of T cells was collected after 48 hours co-culture as mentioned above at 37°C and quantified using Bio-Plex Pro™ Human cytokine Assay (BioRad). Supernatant of *ex vivo* SEB-stimulated CD8⁺ TIL mixture (with confirmed presence of CD94/NKG2A⁺ T cell population) were evaluated using Quantikine human IFN γ or IL2 ELISA kits (R&D Systems), according to manufacturers' instruction. Response was assessed using the abovementioned process of antibody-mediated blocking treatment.

Intracellular cytokine staining

T cell lines were treated with Monensin and Brefeldin A (BD Biosciences) prior to co-culture with peptide-stimulated HLA-E^{high} BCL or HCT116 for another 5 hours at 37°C. Cells were then fixed with Cytofix/Cytoperm™ (BD Biosciences) and stained with conjugated antibodies including Alexa Fluor488-anti-IFN γ (B27; BD Biosciences; RRID:AB_396827), APC-anti-TNF α (Mab-11; Biolegend; RRID:AB_315264), BV421-anti-IL2 (MQ1-17H12, Biolegend; RRID:AB_315264), PE-anti-MIP-1 β (D21-1351; BD Biosciences; RRID:AB_10564091), APC-anti-CD107a (H4A3; BD Biosciences; RRID:AB_1727417). Evaluation of response improvement was assessed using the abovementioned process of antibody-mediated blocking treatment.

CTL killing assay

For the *in vitro* cytotoxicity assay, HLA-E^{high} BCL and HCT116 were stained with 0.5 μ M CFSE before being stimulated by peptides at different concentrations and co-cultured

with antigen-specific T cell lines at 1:1 E:T ratio at 37°C for 6 hours. Cells were then stained with 7-AAD and assessed by the CFSE⁺7-AAD⁻ population present. Evaluation of response was assessed using the abovementioned process of antibody-mediated blocking treatment.

Statistical analysis

All graph generation and statistical analyses were conducted using GraphPad Prism v.7 software. Unless stated otherwise, data are summarized as median \pm s.e.m. All statistical details of experiments can be found in figure legends and results sections. Number of patients used for each analysis are as mentioned in the figure legends. All *in vitro* T cell experiments were performed three times for each type of experiments. Statistically significant differences between two groups were assessed using a two-tailed paired *t*-test, with Wilcoxon adjustments for non-parametrically distributed variable. For comparisons between more than two paired groups of tissues or treatments, one-way ANOVA with Tukey's multiple comparison test was performed. Comparisons between different blocking treatments on different T cell lines and of the difference in TILs populations across different TNM stages were carried out using two-way ANOVA with Tukey's multiple comparisons test. Correlation analysis was performed using non-parametric Spearman test. All tests were two-sided, and differences were considered statistically significant at *p*-value <0.05.

Results

HLA-E expression is upregulated on specific cell populations in tumor

Previous studies have highlighted enrichment of HLA-E across cancer tissue sections (10-13), but it remains uncertain on whether specific cell populations in cancer actually contributed towards the enrichment. We firstly look into whether HLA-E upregulation could be contributed by a specific subpopulation of cancer cells, such as the epithelial cell adhesion molecule (EpCAM)-specific cancer cells, as past studies have demonstrated the commonality of EpCAM overexpression on a majority of carcinomas from tumors of gastrointestinal origin (15, 30-32). Following exclusion of immune cells from our flow cytometry analysis (**Supplementary Fig. S1A**), we confirmed that carcinomas do indeed have EpCAM^{high} cells which are absent in paired paratumor tissue and PBMC, indicating that EpCAM^{high} cells in tumor are specifically epithelial cancer cells (**Fig. 1A**). In addition, the proportion of EpCAM^{dim} tumor-derived cells (average: 50.8%) are lower than the EpCAM^{dim} paratumor-derived cells (average: 74.4%) (**Fig. 1A**), which is consistent with past studies on over-expression of EpCAM on tumor epithelial cells undergoing tumorigenesis and therefore identifying EpCAM^{dim} paratumor cells as normal epithelial cells (15, 30-32).

Upon evaluation of HLA-E on these populations, we observed higher HLA-E⁺ population of EpCAM^{high} epithelial cancer cells (average= 81%), compared to the EpCAM^{dim} tumor-derived cells (average 41.3%) and the EpCAM^{dim} paratumor-derived/tumorigenic epithelial cells (average 21%) (**Fig. 1B**). This is consistent with significantly higher HLA-E surface expression (average MFI=750) observed on the EpCAM^{high} epithelial cancer cells (p<0.01) (**Fig. 1C**). In contrast, MHC-Ia surface expression is downregulated on EpCAM^{high} epithelial cancer cells (**Fig. 1D**). Similar patterns of gradual HLA-E upregulation from EpCAM^{dim} tumor-derived tumorigenic cells to the EpCAM^{high} epithelial

cancer cells were found across different cancers of gastrointestinal origin, namely esophageal, gastric and colorectal cancers (**Supplementary Fig. S1B**).

In addition to cancer cells, the immunosuppressive tumor microenvironment is well known to dysregulate the functionality of tumor-infiltrating immune cells (26-28). We thus decided to assess whether the dysfunctionality could also be due to upregulation of HLA-E expression on macrophages, cDC subsets and plasmacytoid DC (pDC) residing in solid tumors (gating strategy and identification of APC subpopulations as per **Supplementary Fig. S2A and B**). In particular, we found that tumor-localized CD141⁺ cDC have significantly reduced MHC-Ia expression (average of 2-fold to 4-fold) but increased HLA-E expression (average of 2-fold) compared to the same population derived from paired paratumor tissue and PBMC ($r^2 = 0.9747$, $p < 0.01$) (**Fig. 1E**; **Supplementary Fig. S2C**). Other professional APC subsets in tumor, namely CD1c⁺ cDC, pDC and inflammatory macrophages, were also found to have an inverse correlation between the increase in HLA-E expression and the decrease in MHC-Ia expression ($r^2 > 0.9000$, $p < 0.01$) (**Fig. 1E**). Although the frequencies of paratumor-derived and PBMC-derived APC subpopulations were higher, their HLA-E expression was reduced compared to HLA-E expression on the smaller subpopulations of tumor APCs (**Supplementary Fig. S2D**). Non-professional APC such as B cells further demonstrated significant increase of its HLA-E and reduction of MHC-Ia expressions in solid tumors (**Supplementary Fig. S2E**).

A similar pattern of HLA-E upregulation on tumor-derived DCs was observed across the three different cancers of gastrointestinal origin as well as in kidney cancer (**Fig. 1F**). This therefore suggests that HLA-E upregulation is not only enriched on cancer cells but

also on other tumor-residing cells such as on APCs, indicating a potential contributory role of HLA-E in evading anti-tumor cell responses in cancer.

Inhibitory CD94/NKG2A ligand is upregulated on CD8⁺ TILs

Given the upregulation of HLA-E in the tumor microenvironment, we then investigated whether the inhibitory receptor of HLA-E, the heterodimeric CD94/NKG2A, displayed a similar pattern of enrichment in the same set of cancer patients from paired tumor, paratumor and PBMC samples. We observed significant CD94 and NKG2A co-expression and heterodimeric CD94/NKG2A⁺ T cell population in carcinoma, but minimal CD94/NKG2A population and co-expression on T cells derived from paratumor tissue and PBMC (**Fig. 2A and B**). In contrast, we did not observe any heterodimeric CD94/NKG2C⁺ T cell population from tumor, paratumor or PBMC (**Fig. 2C**). The enrichment of CD94/NKG2A⁺ TILs population is directly correlated with the enrichment of HLA-E on both epithelial cancer cells ($r^2=0.9241$, $p<0.001$) and tumor-derived CD141⁺ cDCs on the same cancer patients ($r^2=0.8860$, $p<0.001$) (**Fig. 2D**).

Effector-based immune cells such as CD8⁺ T cells, NKT cells and NK cells were the ones that have significantly higher CD94/NKG2A⁺ population in tumor whereas regulatory-based cells such as CD4⁺ T cells lack any CD94/NKG2A⁺ population in any of the tissue sites evaluated (**Fig. 2E and F**). The enrichment of the CD94/NKG2A⁺ CD8⁺ T cell population in tumor was similarly observed across different types of gastrointestinal cancers, namely esophageal, gastric and colorectal tumors (**Supplementary Fig. S3A**). We observed that gastrointestinal cancer patients with later TNM stage of cancer size (indicative of tumor progression) have a significantly gradual increment of CD94/NKG2A⁺ CD8⁺ TILs population (**Fig. 2G**), suggesting the preferential

selection of CD94/NKG2A and especially HLA-E overexpression during tumor growth in human cancers.

In assessing the maturation phenotype of TILs in tumor, we found that CD94/NKG2A⁺ CD8⁺ TILs are primarily of late stage effector memory phenotype (CD27⁻ CD45RA⁻ CCR7⁻), in contrast to the predominantly early stage effector phenotype of the CD94/NKG2A⁻ population (CD27⁺ CD45RA⁺ CCR7⁻) (**Fig. 2H**). This matured phenotype is characteristic of the tumor-derived CD94/NKG2A⁺ population as the CD94/NKG2A⁺ population from paratumor tissue is primarily early stage effector memory (CD27⁺ CD45RA⁻ CCR7⁻) and the CD94/NKG2A⁺ population from PBMC is mostly early stage central memory phenotype (CD27⁺ CD45RA⁻ CCR7⁺) (**Supplementary Fig. S3B**). The highly matured phenotype of CD94/NKG2A⁺ CD8⁺ TILs population suggest that these TILs in tumor are antigen-experienced T cells that could be selected to upregulate inhibitory CD94/NKG2A expression in order to impair and exhaust antitumor TIL responses.

CD94/NKG2A and PD-1 are co-expressed on CD8⁺ TILs

PD-1^{high} T cells are dysfunctional in solid tumors (33) and thus we evaluated whether the CD94/NKG2A⁺ CD8⁺ TILs could also have high PD-1 expression (**Supplementary Fig. S4**). We found that CD8⁺ TILs are enriched for the PD-1^{high} NKG2A⁺ population whereas the PD-1^{int} TILs have significantly reduced NKG2A co-expression. The PD-1⁻ population lacks CD94/NKG2A expression (**Fig. 3A and B**). Specifically, the PD-1^{high} CD94/NKG2A⁺ population is present in tumors (average of 37% of total CD8⁺ T cells; $p < 0.001$) at a greater frequency, compared to paired paratumor tissue and PBMC (**Fig. 3A and C**).

A similar pattern of PD-1 and CD94/NKG2A co-enrichment on TILs was found in patients with either colorectal or gastric cancers (**Fig. 3D**). In contrast, BTLA and KLRG-1 was found not to be co-expressed on CD94/NKG2A⁺ TILs (**Fig. 3E**), thus suggesting that the exclusive co-expression of CD94/NKG2A with PD-1 in carcinoma and this dual co-expression might contribute to the overall dysfunctionality of PD-1⁺ TILs.

CD94/NKG2A⁺ TILs lack intratumoral CD103 expression

We also found that NKG2A⁺ T cells lack CD103 surface expression such that only the CD94/NKG2A⁻ TILs population are able to express CD103 in tumor ($p < 0.001$) (**Fig. 4A and B**), suggesting antagonistic expression between both markers on TILs. Patients with later TNM stage of cancer size had gradually increasing CD94/NKG2A⁺ CD8⁺ TIL populations but with steadily decreasing CD103⁺ CD8⁺ TIL populations (**Fig. 4C**). This is consistent with the higher CD103⁺ T cell population but a reduced NKG2A⁺ population in paratumor tissue compared to the paired carcinoma (**Fig. 4D**). In comparison to the tissue-localizing CD103⁺ CD94/NKG2A⁺ T cells in PBMC, a significant presence of circulating CD103⁻ CD94/NKG2A⁺ T cells (average=4%) was observed in some cancer patients (**Fig. 4E**), suggesting impaired antitumor cellular responses, which might occur prior to further tumor expansion, also exist in the blood of the cancer patients.

CD94/NKG2A⁺ antigen-specific T cells have impaired proliferation capacity

To investigate the potential role of HLA-E:CD94/NKG2A interaction on immune responses, we isolated CD94/NKG2A⁺ and CD94/NKG2A⁻ populations of PBMC-derived HLA-A2-restricted tumor-associated antigen (TAA)-specific CD8⁺ T cells and co-cultured with HLA-A2-matched allogeneic HCT116 human cancer cell line (HCT116,

which expresses HLA-E at steady-state, **Supplementary Fig. S5A**). We observed reduced proliferation in the CD94/NKG2A⁺ TAA-specific T cell population compared to the CD94/NKG2A⁻ population (60% versus 7%, $p < 0.001$) (**Fig. 5A**). Upon anti-CD94/NKG2A-mediated blocking treatment, most cells of the CD94/NKG2A⁺ population have reduced CFSE expression that is indicative of higher proliferation, compared to the isotype and no blocking treatments (**Fig. 5B**). Similar improvement of proliferation was also observed on tumor-derived antigen-specific T cells following antibody treatment (**Fig. 5C**).

The improvement in T cell proliferation was contributed by the increase in IL2 receptor (CD25) expression on CD94/NKG2A⁺ cells following the antibody blocking treatment, reaching a similarly high receptor expression as of the CD94/NKG2A⁻ population (**Fig. 5D**). This is again observed on the tumor-derived antigen-specific T cells following antibody treatment (**Fig. 5E**). As expected, the upregulation of IL2 receptors (CD25) on the antibody-treated CD94/NKG2A⁺ T cell population corresponded to the increment in IL2 cytokine production and the proportion of IL2-producing cells (**Fig. 5F and G, Supplementary Fig. S5B**). The recovery of IL2 receptor-dependent proliferation following antibody-mediated treatment suggested that enriched HLA-E and CD94/NKG2A interaction on tumor-specific T cells can impair the proliferation capacity, which might subsequently affect its antitumor T cell responses.

Impaired responses recovered after CD94/NKG2A antibody blockade

We next investigated whether the reduced proliferation of CD94/NKG2A⁺ T cells can affect its antitumor killing ability. We found that CD94/NKG2A⁺ population of TAA-specific T cells have poor killing ability when co-cultured with HCT116 cancer cell line

compared to the CD94/NKG2A⁻ population (**Fig. 6A**). The poor killing ability is evident from the significant improvement of cytotoxicity observed on CD94/NKG2A⁺ TAA-specific T cell population when treated with the anti-CD94/NKG2A blocking antibody and is sensitive up to 0.3μM antigen stimulation of HCT116 and up to 0.1μM antigen stimulation of HLA-E^{high} BCL (**Fig. 6B and C**). Similar pattern of T cell cytotoxic recovery was also observed on tumor-derived CD94/NKG2A⁺ antigen-specific T cells, again up to 0.1μM antigen stimulation of HLA-E^{high} BCL (**Fig. 6C**).

In addition, the CD94/NKG2A⁺ TAA-specific T cell population has significantly impaired IFNγ production compared to the CD94/NKG2A⁻ population (**Fig. 6D**). This corresponded to the significantly reduced number of IFNγ-expressing cells of the CD94/NKG2A⁺ population, when co-cultured with either HCT116 or HLA-E^{high} BCL, even at high antigen stimulation of 1 μM (**Fig. 6E**). Similar to the recovery in proliferation and cytotoxicity, IFNγ production and expression recovered following anti-CD94/NKG2A-mediated blockade treatment (**Fig. 6F and G, Supplementary Fig. S5B**). However, no differences were observed in TNFα and MIP-1β responses following the anti-CD94/NKG2A blockade treatment. Only the chemotactic CCL5 was significantly elevated 48 hours later (**Supplementary Fig. S6A to G**). Taken altogether, these *in vitro* data suggest that enriched HLA-E and CD94/NKG2A interaction, particularly on tumor-specific T cells, affected the survivability of T cells through their proliferation capacity, antitumor cytotoxicity and cytokine responses.

To corroborate the *in vitro* observations, we then set up an *ex vivo* study by isolating cell mixtures from tumors of four gastric cancer patients with confirmed presence of at least

5% of CD94/NKG2A⁺ TILs and stimulated with SEB before being treated with anti-CD94/NKG2A blocking antibody. Consistent with our *in vitro* findings, we confirmed that the frequency of IFN γ -expressing cells and the amount of IFN γ produced were significantly improved following antibody-mediated treatment compared to the isotype and no blocking treatments (**Fig. 7A and B, Supplementary Fig. S7**). Furthermore, more stages of cell proliferation were observed after the anti-CD94/NKG2A blocking treatment (**Fig. 7 C**), corresponding to significantly elevated IL2 receptor (CD25) expression on CD8⁺ TILs 48 hours later (**Fig. 7 D**). The IL2 receptor-dependent proliferation was vital in the recovery of CD8⁺ TILs *ex vivo* after antibody treatment, as the IL2 expression and production were also found to be significantly elevated on CD8⁺ TILs (**Fig. 7E and F, Supplementary Fig. S7**).

Altogether, our *in vitro* and *ex vivo* observations indicated that the enriched presence and interaction between HLA-E and CD94/NKG2A, particularly on tumor-specific T cells, can negatively affect antitumor T cell immune responses and contribute to the exhaustive and dysfunctional nature of TILs in gastrointestinal cancer patients.

Discussion

Using comparison between paired tumor, paratumor and PBMC from mainly gastrointestinal cancer patients, we reported on enrichment of HLA-E in carcinoma that is contributed not only by the epithelial cancer cells but also by tumor dendritic cells and macrophages. The HLA-E enrichment paralleled the increment in the inhibitory CD94/NKG2A⁺ CD8⁺ TIL population that is exclusively associated with PD-1^{high}

expression in solid tumors, but minimally present in paired paratumor tissue and absent in PBMC of cancer patients.

Studies by Andre and colleagues as well as by van Manfoort and colleagues highlighted the improvement in survival rates and tumor control in anti-NKG2A-treated murine cancer models and the increased disease stability of combinatory anti-NKG2A and anti-EGFR-treated head-and-neck cancer patients of a phase II clinical trial (12, 13). Our current study reveals mechanisms by which enriched presence and interaction of HLA-E with CD94/NKG2A could impair antitumor T cell responses in human cancer. The improvement of IL2 receptor-dependent proliferation and antitumor killing by tumor-specific T cells treated with anti-CD94/NKG2A revealed the inhibitory effect of enriched CD94/NKG2A presence on human TILs, which contribute towards worse clinical outcomes in patients as tumor progresses.

In addition, past studies indicating abundance of HLA-E in cross-sectional cancer tissue analysis lack corresponding comparison with paired paratumor tissue and blood of the patients and did not examine the types of cells that contribute to this abundance. Here, , we showed that HLA-E enrichment occurs on epithelial cancer cells and on tumor-residing APCs. Tumor-residing APCs help in tissue-localized antigen presentation and maintenance of antitumor T cell responses (20-22). However, other murine studies have also shown that tumor APCs can be dysregulated to become tolerogenic, a process driven by immunosuppressive factors such as IL10 and β -catenin (26, 27, 34, 35). For instance, the inhibitory PD-1/PD-L1 axis was upregulated on murine tumor APC and contributed to progressively growing tumor (28, 36, 37). We further demonstrated that not only can HLA-E be upregulated on tumor-residing APC, but its inhibitory

CD94/NKG2A ligand on TILs is also upregulated within larger tumors. This in turn could elucidate the reasons that past DC-based vaccines that solely targeted recovery of tumor neoantigen presentation on MHC-Ia of tumor DC were not successful at improving recovery in murine cancer models and cancer patients (23-25). The enriched HLA-E and CD94/NKG2A presence and interaction between tumor-APCs and CD8⁺ TILs could overpower and dampen the activating MHC Class Ia-T cell receptor signaling, causing ineffective antitumor priming and anergic T cell activation.

The corresponding increment of CD94/NKG2A on TILs in gastrointestinal cancer patients is antagonistic to the downregulation of the intratumoral CD103 expression. CD103⁺ T cells are T cell mediators of long-lived protection against viral infections in peripheral tissues such as intestines and lung (38, 39). In the cancer setting, the presence of CD103 aids T cell infiltration into intraepithelial murine tumors whereas the accumulation of CD103 contributed to extensive granzyme B degranulation in the immunological synapse, leading to better killing of cancer cells *in vitro* (40, 41). The observation of gradual loss of CD103 in progressively growing gastrointestinal tumors suggests that CD103 absence is detrimental towards cancer survival and that cancer preferentially upregulates inhibitory markers such as CD94/NKG2A and PD-1 expression as a mechanism to avoid antitumor immunity. Our observation of antagonistic expression is contradictory to the co-expression of NKG2A with CD103 on TILs observed by van Manfoort and colleagues on human papilloma virus (HPV)-positive cervical carcinoma patients (13). It is most likely that any NKG2A co-expression with CD103 could be present on viral-specific tumor-infiltrating T lymphocytes, whereby another study has highlighted the over-abundance of bystander viral-specific T cells in

tumor that do not recognize tumor neoantigens and therefore might not have antitumor immune capacity in carcinoma (42).

Patients with PD-1^{high} T cells have demonstrated good responses to anti-PD-1 treatment due to their impaired functionality and characteristics (33). Although anti-PD-1 treatment in various clinical studies has supported recovery towards prolonged survival in cancer patients, there is still a sizeable portion of patients that lacked major improvement (6, 7). We demonstrated here that PD-1^{high} TILs in gastrointestinal cancer patients have enriched CD94/NKG2A expression, which is consistent with findings in studies in head-and-neck cancer patients (12, 13). As we further show that the enriched CD94/NKG2A⁺ tumor-specific T cells lack efficient proliferation capacity, this can therefore lead to detrimental outcome on the long-term survivability of antitumor T cells. Subsequently, the reduced proliferation of TILs could eventually contribute towards the impaired antitumor cytotoxicity and responses against cancer, albeit even after being treated with anti-PD-1 treatment. The commonality of HLA-E and CD94/NKG2A enrichment across different cancer types, together with the exclusivity of PD-1^{high} expression highlights the key role of CD94/NKG2A as a compensatory exhaustive marker of TILs that limits the effectiveness of antitumor TILs.

In light of cancer immunotherapy, targeting the inhibitory CD94/NKG2A signaling pathways on TILs and their interaction with HLA-E in tumors could prove beneficial to patients with HLA-E and PD-1 enriched tumors. Targeting CD94/NKG2A could improve the long-term survivability of effector cells such as CD8⁺ T cells with better cytotoxic functions following combinatory anti-PD-1 treatment, especially in early stage cancer patients.

Author contributions

Conceptualization and Methodology, M.A.H., R.W., X.Y., Y.P., A.M., and T.D.;

Formal analysis, M.A.H., X.L. and Y.P.;

Investigation, M.A.H., X.Y., P.F., X.C., Y.F., C.W. and Y.P.;

Resources, R.W., S.J., C.V., D.M.P., C.W., A.S., C.C., X.W. and T.D.;

Writing- original draft, M.A.H., R.W., Y.P. and T.D.;

Visualization & Writing- Review & Editing, M.A.H., R.W., V.C., A.M., X.W., Y.P. and T.D.

Acknowledgements

This work was supported by the Chinese Academy of Medical Sciences (CAMS) Innovation Fund for Medical Sciences (CIFMS), China (grant number: 2018-I2M-2-002 and 2017PT31043); Medical Research Council, United Kingdom (MR/L018942/1 and MRC Human Immunology Unit Core). MAH is funded by the Malaysia's King Scholarship, CV research time is supported by the National Institute of Health Research (NIHR) Oxford Biomedical Research Centre (BRC) (Molecular Diagnostics Theme/Multimodal Pathology Subtheme); DMP is funded by the NIHR Oxford BRC (Molecular Diagnostics Theme/Multimodal Pathology Subtheme).

We thank Oxford Radcliffe Biobank and Xinjiang Tumor Hospital Biobank for the samples provided, Djamilia Ouaret for the information on EpCAM-specific cancer cells, Timothy Powell for assistance and Alain Townsend for his advices throughout the study.

The authors declare no competing financial interests

References

1. Koopman LA, Corver WE, van der Slik AR, Giphart MJ, Fleuren GJ. Multiple genetic alterations cause frequent and heterogeneous human histocompatibility leukocyte antigen class I loss in cervical cancer. *J Exp Med*. 2000;191(6):961-76.
2. Ahmadzadeh M, Johnson LA, Heemskerk B, Wunderlich JR, Dudley ME, White DE, et al. Tumor antigen-specific CD8 T cells infiltrating the tumor express high levels of PD-1 and are functionally impaired. *Blood*. 2009;114(8):1537-44.
3. Leone P, Shin EC, Perosa F, Vacca A, Dammacco F, Racanelli V. MHC class I antigen processing and presenting machinery: organization, function, and defects in tumor cells. *J Natl Cancer Inst*. 2013;105(16):1172-87.
4. Wolchok JD, Neyns B, Linette G, Negrier S, Lutzky J, Thomas L, et al. Ipilimumab monotherapy in patients with pretreated advanced melanoma: a randomised, double-blind, multicentre, phase 2, dose-ranging study. *Lancet Oncol*. 2010;11(2):155-64.
5. Besser MJ, Shapira-Frommer R, Itzhaki O, Treves AJ, Zippel DB, Levy D, et al. Adoptive transfer of tumor-infiltrating lymphocytes in patients with metastatic melanoma: intent-to-treat analysis and efficacy after failure to prior immunotherapies. *Clin Cancer Res*. 2013;19(17):4792-800.
6. Garon EB, Rizvi NA, Hui R, Leighl N, Balmanoukian AS, Eder JP, et al. Pembrolizumab for the treatment of non-small-cell lung cancer. *N Engl J Med*. 2015;372(21):2018-28.

7. Muro K, Chung HC, Shankaran V, Geva R, Catenacci D, Gupta S, et al. Pembrolizumab for patients with PD-L1-positive advanced gastric cancer (KEYNOTE-012): a multicentre, open-label, phase 1b trial. *Lancet Oncol.* 2016;17(6):717-26.
8. Levy EM, Bianchini M, Von Euw EM, Barrio MM, Bravo AI, Furman D, et al. Human leukocyte antigen-E protein is overexpressed in primary human colorectal cancer. *Int J Oncol.* 2008;32(3):633-41.
9. de Kruif EM, Sajet A, van Nes JG, Natanov R, Putter H, Smit VT, et al. HLA-E and HLA-G expression in classical HLA class I-negative tumors is of prognostic value for clinical outcome of early breast cancer patients. *J Immunol.* 2010;185(12):7452-9.
10. Gooden M, Lampen M, Jordanova ES, Leffers N, Trimpos JB, van der Burg SH, et al. HLA-E expression by gynecological cancers restrains tumor-infiltrating CD8(+) T lymphocytes. *Proc Natl Acad Sci U S A.* 2011;108(26):10656-61.
11. Bossard C, Bezieau S, Matysiak-Budnik T, Volteau C, Laboisie CL, Jotereau F, et al. HLA-E/beta2 microglobulin overexpression in colorectal cancer is associated with recruitment of inhibitory immune cells and tumor progression. *Int J Cancer.* 2012;131(4):855-63.
12. Andre P, Denis C, Soulas C, Bourbon-Caillet C, Lopez J, Arnoux T, et al. Anti-NKG2A mAb Is a Checkpoint Inhibitor that Promotes Anti-tumor Immunity by Unleashing Both T and NK Cells. *Cell.* 2018;175(7):1731-43 e13.
13. van Montfoort N, Borst L, Korrer MJ, Sluijter M, Marijt KA, Santegoets SJ, et al. NKG2A Blockade Potentiates CD8 T Cell Immunity Induced by Cancer Vaccines. *Cell.* 2018;175(7):1744-55 e15.

14. Braud VM, Allan DS, O'Callaghan CA, Soderstrom K, D'Andrea A, Ogg GS, et al. HLA-E binds to natural killer cell receptors CD94/NKG2A, B and C. *Nature*. 1998;391(6669):795-9.
15. Lazetic S, Chang C, Houchins JP, Lanier LL, Phillips JH. Human natural killer cell receptors involved in MHC class I recognition are disulfide-linked heterodimers of CD94 and NKG2 subunits. *J Immunol*. 1996;157(11):4741-5.
16. Lee N, Llano M, Carretero M, Ishitani A, Navarro F, Lopez-Botet M, et al. HLA-E is a major ligand for the natural killer inhibitory receptor CD94/NKG2A. *Proc Natl Acad Sci U S A*. 1998;95(9):5199-204.
17. Tomasec P, Braud VM, Rickards C, Powell MB, McSharry BP, Gadola S, et al. Surface expression of HLA-E, an inhibitor of natural killer cells, enhanced by human cytomegalovirus gpUL40. *Science*. 2000;287(5455):1031.
18. Ulbrecht M, Martinozzi S, Grzeschik M, Hengel H, Ellwart JW, Pla M, et al. Cutting edge: the human cytomegalovirus UL40 gene product contains a ligand for HLA-E and prevents NK cell-mediated lysis. *J Immunol*. 2000;164(10):5019-22.
19. Braud VM, Aldemir H, Breart B, Ferlin WG. Expression of CD94-NKG2A inhibitory receptor is restricted to a subset of CD8⁺ T cells. *Trends Immunol*. 2003;24(4):162-4.
20. Bachem A, Guttler S, Hartung E, Ebstein F, Schaefer M, Tannert A, et al. Superior antigen cross-presentation and XCR1 expression define human CD11c⁺CD141⁺ cells as homologues of mouse CD8⁺ dendritic cells. *J Exp Med*. 2010;207(6):1273-81.

21. Roberts EW, Broz ML, Binnewies M, Headley MB, Nelson AE, Wolf DM, et al. Critical Role for CD103(+)/CD141(+) Dendritic Cells Bearing CCR7 for Tumor Antigen Trafficking and Priming of T Cell Immunity in Melanoma. *Cancer Cell*. 2016;30(2):324-36.
22. Tseng D, Volkmer JP, Willingham SB, Contreras-Trujillo H, Fathman JW, Fernhoff NB, et al. Anti-CD47 antibody-mediated phagocytosis of cancer by macrophages primes an effective antitumor T-cell response. *Proc Natl Acad Sci U S A*. 2013;110(27):11103-8.
23. Kavanagh B, Ko A, Venook A, Margolin K, Zeh H, Lotze M, et al. Vaccination of metastatic colorectal cancer patients with matured dendritic cells loaded with multiple major histocompatibility complex class I peptides. *J Immunother*. 2007;30(7):762-72.
24. Slingluff CL, Jr., Petroni GR, Chianese-Bullock KA, Smolkin ME, Hibbitts S, Murphy C, et al. Immunologic and clinical outcomes of a randomized phase II trial of two multi-peptide vaccines for melanoma in the adjuvant setting. *Clin Cancer Res*. 2007;13(21):6386-95.
25. Iversen TZ, Engell-Noerregaard L, Ellebaek E, Andersen R, Larsen SK, Bjoern J, et al. Long-lasting disease stabilization in the absence of toxicity in metastatic lung cancer patients vaccinated with an epitope derived from indoleamine 2,3 dioxygenase. *Clin Cancer Res*. 2014;20(1):221-32.
26. Ruffell B, Chang-Strachan D, Chan V, Rosenbusch A, Ho CM, Pryer N, et al. Macrophage IL-10 blocks CD8+ T cell-dependent responses to chemotherapy by suppressing IL-12 expression in intratumoral dendritic cells. *Cancer Cell*. 2014;26(5):623-37.

27. Laoui D, Keirsse J, Morias Y, Van Overmeire E, Geeraerts X, Elkrim Y, et al. The tumour microenvironment harbours ontogenically distinct dendritic cell populations with opposing effects on tumour immunity. *Nat Commun.* 2016;7:13720.
28. Salmon H, Idoyaga J, Rahman A, Leboeuf M, Remark R, Jordan S, et al. Expansion and Activation of CD103(+) Dendritic Cell Progenitors at the Tumor Site Enhances Tumor Responses to Therapeutic PD-L1 and BRAF Inhibition. *Immunity.* 2016;44(4):924-38.
29. Zhang C, Peng Y, Hublitz P, Zhang H, Dong T. Genetic abrogation of immune checkpoints in antigen-specific cytotoxic T-lymphocyte as a potential alternative to blockade immunotherapy. *Sci Rep.* 2018;8(1):5549.
30. Osta WA, Chen Y, Mikhitarian K, Mitas M, Salem M, Hannun YA, et al. EpCAM is overexpressed in breast cancer and is a potential target for breast cancer gene therapy. *Cancer Res.* 2004;64(16):5818-24.
31. El-Sahwi K, Bellone S, Cocco E, Casagrande F, Bellone M, Abu-Khalaf M, et al. Overexpression of EpCAM in uterine serous papillary carcinoma: implications for EpCAM-specific immunotherapy with human monoclonal antibody adecatumumab (MT201). *Mol Cancer Ther.* 2010;9(1):57-66.
32. Kuiper RP, Vissers LE, Venkatachalam R, Bodmer D, Hoenselaar E, Goossens M, et al. Recurrence and variability of germline EPCAM deletions in Lynch syndrome. *Hum Mutat.* 2011;32(4):407-14.
33. Thommen DS, Koelzer VH, Herzig P, Roller A, Trefny M, Dimeloe S, et al. A transcriptionally and functionally distinct PD-1(+) CD8(+) T cell pool with predictive

potential in non-small-cell lung cancer treated with PD-1 blockade. *Nat Med*. 2018;24(7):994-1004.

34. Spranger S, Bao R, Gajewski TF. Melanoma-intrinsic beta-catenin signalling prevents anti-tumour immunity. *Nature*. 2015;523(7559):231-5.

35. Scarlett UK, Rutkowski MR, Rauwerdink AM, Fields J, Escovar-Fadul X, Baird J, et al. Ovarian cancer progression is controlled by phenotypic changes in dendritic cells. *J Exp Med*. 2012;209(3):495-506.

36. Hildner K, Edelson BT, Purtha WE, Diamond M, Matsushita H, Kohyama M, et al. Batf3 deficiency reveals a critical role for CD8alpha+ dendritic cells in cytotoxic T cell immunity. *Science*. 2008;322(5904):1097-100.

37. Okazaki T, Chikuma S, Iwai Y, Fagarasan S, Honjo T. A rheostat for immune responses: the unique properties of PD-1 and their advantages for clinical application. *Nat Immunol*. 2013;14(12):1212-8.

38. Gebhardt T, Wakim LM, Eidsmo L, Reading PC, Heath WR, Carbone FR. Memory T cells in nonlymphoid tissue that provide enhanced local immunity during infection with herpes simplex virus. *Nat Immunol*. 2009;10(5):524-30.

39. Masopust D, Choo D, Vezys V, Wherry EJ, Duraiswamy J, Akondy R, et al. Dynamic T cell migration program provides resident memory within intestinal epithelium. *J Exp Med*. 2010;207(3):553-64.

40. Le Floc'h A, Jalil A, Vergnon I, Le Maux Chansac B, Lazar V, Bismuth G, et al. Alpha E beta 7 integrin interaction with E-cadherin promotes antitumor CTL activity by triggering lytic granule polarization and exocytosis. *J Exp Med*. 2007;204(3):559-70.

41. Djenidi F, Adam J, Goubar A, Durgeau A, Meurice G, de Montpreville V, et al. CD8+CD103+ tumor-infiltrating lymphocytes are tumor-specific tissue-resident memory T cells and a prognostic factor for survival in lung cancer patients. *J Immunol*. 2015;194(7):3475-86.
42. Simoni Y, Becht E, Fehlings M, Loh CY, Koo SL, Teng KWW, et al. Bystander CD8(+) T cells are abundant and phenotypically distinct in human tumour infiltrates. *Nature*. 2018;557(7706):575-9.

Figure legends

Figure 1. Epithelial-derived cancer cells and tumor-residing antigen-presenting cells have higher HLA-E expression but reduced MHC-1a expression. (A)

Representative contour plots of EpCAM expression on cells isolated from paired tumor, paratumor and PBMC, with EpCAM^{high} cells observed only in tumor-derived tissue identified as epithelial cancer cells whereas EpCAM^{dim} tumor-derived cells as tumorigenic cells and EpCAM^{dim} paratumor-derived cells as normal epithelial cells. (B) Representative gating of HLA-E⁺ population on tumor-derived EpCAM^{high} cancer cells (*left*), tumor-derived EpCAM^{dim} tumorigenic cells (*middle*) and paratumor-derived EpCAM^{dim} normal epithelial cells (*right*). The HLA-E expression (C) and MHC-1a expression (D) by median fluorescence intensity (MFI) on three different populations of EpCAM-expressing populations. N, number of patients=10 (esophageal cancer, n=3, gastric cancer, n=4, colorectal cancer, n=3); one-way ANOVA with Tukey's post hoc analysis, F-values, degree of freedom: 5.852,9 (*left*); 4.163,9 (*right*). (E) Correlative expression of HLA-E and MHC-1a by MFI on CD141⁺ cDC, CD1c⁺ cDC, pDC and

inflammatory macrophages derived from paired tumor, paratumor and PBMC. N, number of patients=22 (esophageal cancer, n=7, gastric cancer, n=8, colorectal cancer, n=7); correlative analysis of non-parametric Spearman test, $r^2 = 0.9747$ $p < 0.01$ for CD141+ cDC; $r^2 = 0.8174$ $p < 0.05$ for CD1c+ cDC; $r^2 = 0.9764$ $p < 0.01$ for pDC; $r^2 = 0.9085$ $p < 0.01$ for inflammatory macrophages. (F) HLA-E expression by MFI on DC subsets from paired tumor, paratumor and PBMC samples in four different cancer types. (N, number of esophageal cancer patients=7; gastric cancer n=8; colorectal cancer n=7; kidney cancer n=5).; one-way ANOVA with Tukey's post hoc analysis. Horizontal line represents median; interval represent 95% confidence. Connecting lines represents samples from the same patients. * indicates p -value <0.05 , ** p -values <0.01 , *** p -values <0.001 , ns, not significant. Data represent with median \pm s.e.m.

Figure 2. CD94/NKG2A expression and presence is higher on tumor-infiltrating immune cells. (A) Representative contour plots on CD94 and NKG2A staining on CD3⁺ T cells from paired tumor, paratumor and PBMC samples from one cancer patient (Proportion of CD94/NKG2A⁺ T cells in tumor=17.9%; in paratumor=1.27%; in PBMC=0.3%). (B) Correlative analysis on NKG2A and CD94 expression by MFI on tumor-derived CD3⁺ T cells. N, number of patients= 22 (esophageal cancer, n=7, gastric cancer, n=8, colorectal cancer, n=7); correlative analysis of non-parametric Spearman test, $r^2 = 0.9064$ $p < 0.001$. (C) The frequency of CD94/NKG2C⁺ T cells from paired tumor, paratumor and PBMC samples. N, number of patients=22 (esophageal cancer, n=7, gastric cancer, n=8, colorectal cancer, n=7). (D) Correlative analysis between the frequency of CD94/NKG2A⁺ CD3⁺ TILs with the HLA-E expression by MFI on EpCAM-specific tumor cells (*left*) and the HLA-E expression by MFI on tumor-derived CD141⁺

cDC (*right*). N, number of patients= 10 (esophageal cancer, n=3, gastric cancer, n=4, colorectal cancer, n=3); correlative analysis of non-parametric Spearman test, $r^2=0.9241$ $p<0.0001$ (*left*); $r^2=0.8860$ $p<0.0001$ (*right*). (E) The proportion of CD94/NKG2A⁺ populations of CD3⁺ T cells, CD8⁺ T cells, NKT cells and NK cells from paired tumor, paratumor and PBMC. N, number of patients=22 (esophageal cancer, n=7, gastric cancer, n=8, colorectal cancer, n=7); one-way ANOVA with Tukey's post hoc analysis. (F) The proportion of CD94/NKG2A⁺ population of CD4⁺ T cells derived from paired tumor, paratumor and PBMC. N, number of patients=22 (esophageal cancer, n=7, gastric cancer, n=8, colorectal cancer, n=7). (G) The proportion of CD94/NKG2A⁺ and CD94/NKG2A⁻ populations of CD8⁺ TILs according to TNM stage of clinical prognosis. N, number of patients =22; (esophageal carcinoma, n=7, gastric carcinoma, n=8, colorectal carcinoma, n=7); two-way ANOVA with Tukey's post hoc analysis. (H) The proportion of CD94/NKG2A⁺ CD8⁺ TILs (*left*), CD94/NKG2A⁻ CD8⁺ TILs (*middle*) and total CD8⁺ TILs (*right*) according to maturation phenotype expression of CD27, CD45RA and CCR7 in carcinoma. (N, number of patients =22; (esophageal carcinoma, n=7, gastric carcinoma, n=8, colorectal carcinoma, n=7); one-way ANOVA with Tukey's post hoc analysis. Horizontal line represents median; interval represent 95% confidence. Connecting lines represents samples from the same patients * indicates $p\text{-value}<0.05$, ** $p\text{-values}<0.01$, *** $p\text{-values}<0.001$, ns, not significant. Data represent with median \pm s.e.m.

Figure 3. CD94/NKG2A⁺ TILs exclusively co-expressed PD-1. (A) Representative contour plots of PD-1 and NKG2A expression on CD8⁺ T cells derived from paired tumor, paratumor and PBMC, according to PD-1 high, intermediate or negative

expression (B) The proportion of CD94/NKG2A⁺ CD8⁺ TILs expressing either PD-1^{high}, PD-1^{int} or PD-1⁻. N, number of patients=22 (esophageal cancer, n=5, gastric cancer, n=6, colorectal cancer, n=6, lung cancer, n=5); one-way ANOVA with Tukey's post hoc analysis. (C) Proportion of CD94/NKG2A⁺ PD-1^{high} CD8⁺ T cells from paired tumor, paratumor and PBMC. N, number of patients=22 (esophageal cancer, n=7, gastric cancer, n=8, colorectal cancer, n=7); one-way ANOVA with Tukey's post hoc analysis. (D) The proportion of CD94/NKG2A⁺ PD-1^{high} CD8⁺ T cells from paired tumor, paratumor and PBMC according to cancer types; colorectal cancer patients n=7 (*left*) and gastric cancer patients n=8 (*right*); one-way ANOVA with Tukey's post hoc analysis. (E) Proportion of CD94/NKG2A⁺ CD8⁺ TILs expressing either BTLA, KLRG-1 or PD-1 according to cancer types; colorectal cancer patients n=7 (*left*) and gastric cancer patients n=8 (*right*). Horizontal line represents median; interval represent 95% confidence. Connecting lines represents samples from the same patients * indicates p-value<0.05, ** p-values<0.01, *** p-values<0.001, ns, not significant. Data represent with median±s.e.m.

Figure 4. CD94/NKG2A⁺ TILs lack tissue resident CD103 marker. (A) Representative FACS plot on NKG2A and CD103 expression on CD8⁺ T cells derived from paired tumor, paratumor and PBMC, by MFI and proportion of CD103⁺ NKG2A⁻ population. (B) Proportion of CD103⁺ CD8⁺ TILs being either CD94/NKG2A⁺ or CD94/NKG2A⁻. N, number of patients=10; (esophageal carcinoma, n=2, gastric carcinoma, n=2, colorectal carcinoma, n=3, lung carcinoma, n=3); paired student *t* test with Wilcoxon adjustments, F-values, degree of freedom: 12.64,9. (C) The proportion of CD94/NKG2A⁺ CD103⁻ and CD94/NKG2A⁻ CD103⁺ populations on CD8⁺ TILs according to TNM stage of clinical

prognosis. N, number of patients=10; (esophageal carcinoma, n=2, gastric carcinoma, n=2, colorectal carcinoma, n=3, lung carcinoma, n=3); two-way ANOVA with Tukey's post-hoc analysis. (D) The proportion of CD103⁺ and CD94/NKG2A⁺ populations of CD3⁺ T cells derived from paired tumor and paratumor tissue. N, number of patients=10; F-values, (esophageal carcinoma, n=2, gastric carcinoma, n=2, colorectal carcinoma, n=3, lung carcinoma, n=3); paired student *t* test with Wilcoxon adjustments, degree of freedom: 7.364,9 (*left*); 6.938,9 (*right*). (E) The proportion of circulating CD8⁺ T cells (CD94/NKG2A⁺ CD103⁻) and tissue-homing CD8⁺ T cells (CD94/NKG2A⁺ CD103⁺) from PBMC. N, number of patients=10; (esophageal carcinoma, n=2, gastric carcinoma, n=2, colorectal carcinoma, n=3, lung carcinoma, n=3); paired student *t* test with Wilcoxon adjustments, F-values, degree of freedom: 4.556,9. Horizontal line represents median; interval represent 95% confidence. * indicates p-value<0.05, ** p-values<0.01, *** p-values<0.001, ns, not significant. Data represent with median±s.e.m.

Figure 5. CD94/NKG2A⁺ HLA-A2-restricted antigen-specific T cells have impaired proliferation which recovers following antibody-mediated blocking treatment *in vitro*. (A) The proportion of proliferating cells of CD94/NKG2A⁺ or CD94/NKG2A⁻ TAA-specific T cells following co-cultured with HCT116. N, number of experimental repeats, n=3; Paired student t-test with Wilcoxon adjustments; F-values, degree of freedom: 117.8,2. (B) Representative histogram plots of CFSE-based proliferating cells of CD94/NKG2A⁺ (*left*) and CD94/NKG2A⁻ (*right*) TAA-specific T cells following three different treatments. (C) The proportion of proliferating cells on PBMC-derived TAA-specific T cells and tumor-derived CMV-specific T cells following three different treatments. N, number of experimental repeats=3; one-way ANOVA with Tukey's post

hoc analysis. (D) Representative histogram plots of IL2 receptor (CD25) expression by MFI on CD94/NKG2A⁺ (*left*) and CD94/NKG2A⁻ (*right*) TAA-specific T cells following three different treatments. IL2 receptor (CD25) expression by MFI (E), IL2 production (F) and IL2⁺ cells proportion (G) on PBMC-derived TAA-specific T cells and tumor-derived CMV-specific T cells following three different treatments. N, number of experimental repeats=3; one-way ANOVA with Tukey's post hoc analysis.. P value represent 95% confidence. * indicates p-value<0.05, ** p-values<0.01, *** p-values<0.001, ns, not significant. Data represent with median±s.e.m.

Figure 6. Impairment of IFN γ response and cytotoxicity by CD94/NKG2A⁺ HLA-A2-restricted antigen-specific T cells which recovers following antibody-mediated blocking treatment *in vitro*. (A) The proportion of lysed cancer cells following CD94/NKG2A⁺ or CD94/NKG2A⁻ TAA-specific T cells co-cultured with HCT116. N, number of experimental repeats, n=3; Paired student t-test with Wilcoxon adjustments; F-values, degree of freedom: 47.3,2. (B) The proportion of lysed cancer cells following CD94/NKG2A⁺ TAA-specific T cell population co-culture with HCT116, following either CD94/NKG2A antibody blockade, isotype or no blocking treatments at five different concentration of antigen stimulation. N, number of experimental repeats, n=3; two-way ANOVA with Tukey's post hoc analysis. (C) The proportion of lysed cancer cells following co-culture of CD94/NKG2A⁺ population of PBMC-derived TAA-specific T cells (*left*) and tumor-derived CMV-specific T cells (*right*) with HLA-E^{high} BCL. N, number of experimental repeats, n=3; two-way ANOVA with Tukey's post hoc analysis. (D) The IFN γ production of CD94/NKG2A⁺ or CD94/NKG2A⁻ TAA-specific T cells following co-cultured with HLA-A2-matched HLA-E^{high} BCL. N, number of experimental repeats, n=3;

Paired student t-test with Wilcoxon adjustments; F-values, degree of freedom: 33.9,2.

(E) The proportion of IFN γ ⁺ cells of CD94/NKG2A⁺ or CD94/NKG2A⁻ TAA-specific T cells following co-culture with either HCT116 or HLA-E^{high} BCL N, number of experimental repeats, n=3; Paired student t-test with Wilcoxon adjustments. The proportion of IFN γ ⁺ cells (F) and IFN γ production (G) of CD94/NKG2A⁺ population of PBMC-derived TAA-specific T cells and tumor-derived CMV-specific T cells following either CD94/aNKG2A antibody blockade, isotype or no blocking treatments. N, number of experimental repeats, n=3; one-way ANOVA with Tukey's post hoc analysis. P value represent 95% confidence. * indicates p-value<0.05, ** p-values<0.01, *** p-values<0.001, ns, not significant. Data represent with median \pm s.e.m.

Figure 7. Recovery of CD8⁺ TILs functions following anti-CD94/NKG2A-mediated blocking treatment *ex vivo*. The proportion of IFN γ ⁺ cells (A) and IFN γ production (B) of CD8⁺ TILs stimulated with 0.1 μ M SEB stimulation following either CD94/aNKG2A antibody blockade, isotype or no blocking treatment. N, number of gastric cancer patients, n=4; one-way ANOVA with Tukey's post hoc analysis. (C) Representative histogram plot of CFSE-based proliferating cells of CD8⁺ TILs following different treatments. The IL2 receptor (CD25) geometric MFI expression (D), proportion of IL2⁺ cells (E) and IL2 production (F) on CD8⁺ TILs following different treatments. N, number of gastric cancer patients, n=4; one-way ANOVA with Tukey's post hoc analysis. P value represent 95% confidence. * indicates p-value<0.05, ** p-values<0.01, *** p-values<0.001, ns, not significant. Data represent with median \pm s.e.m.

Figure 1

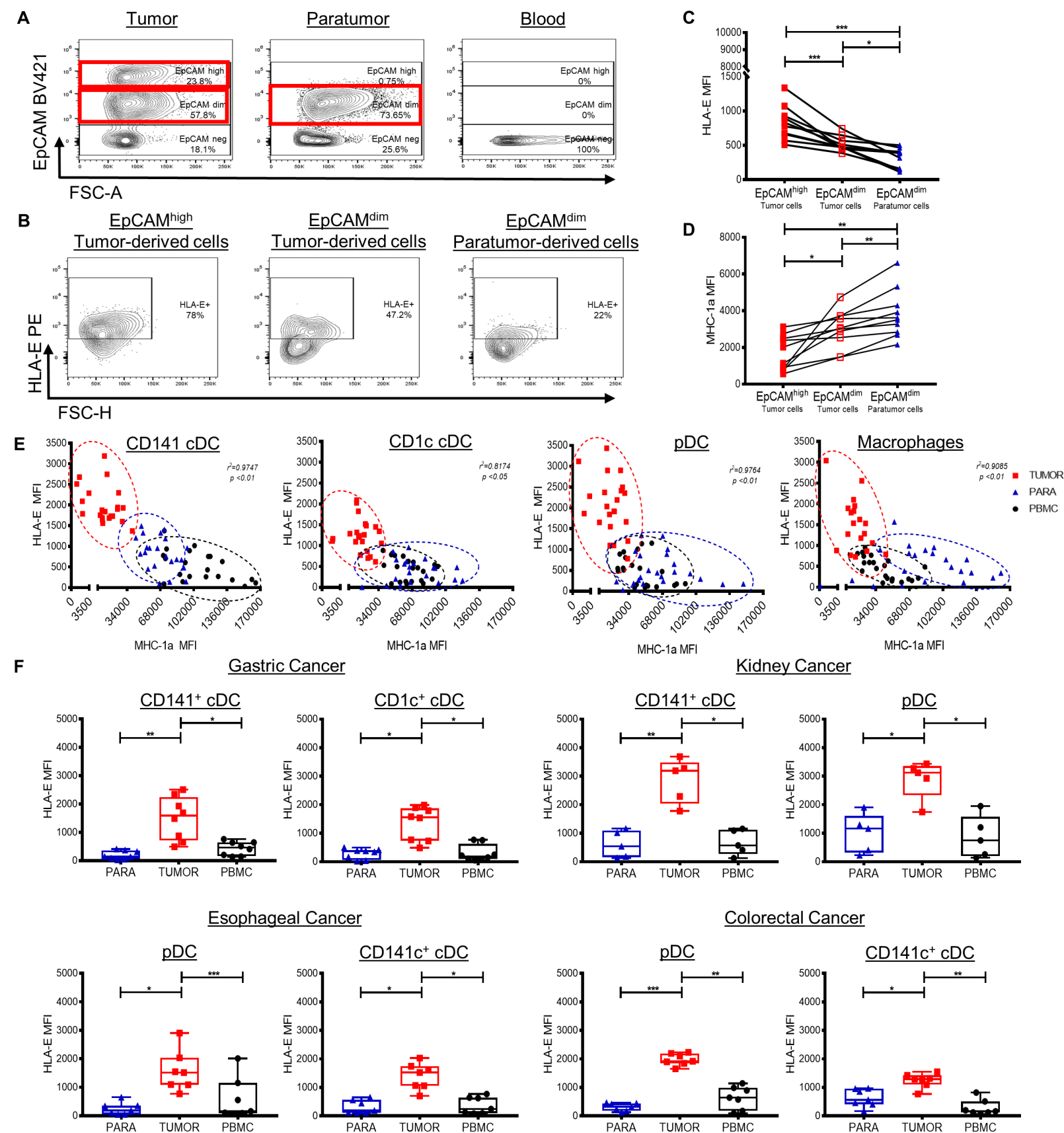
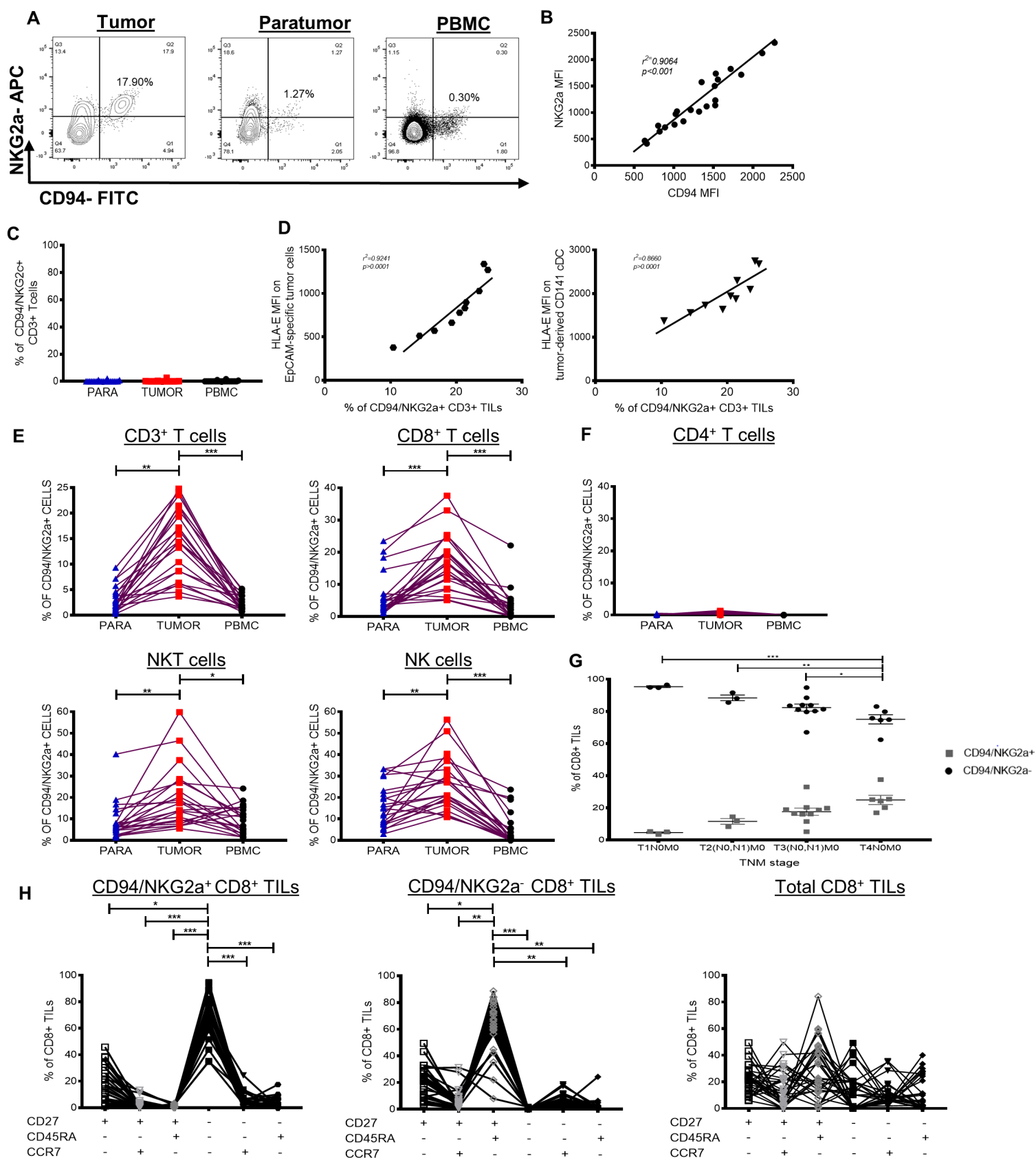


Figure 2



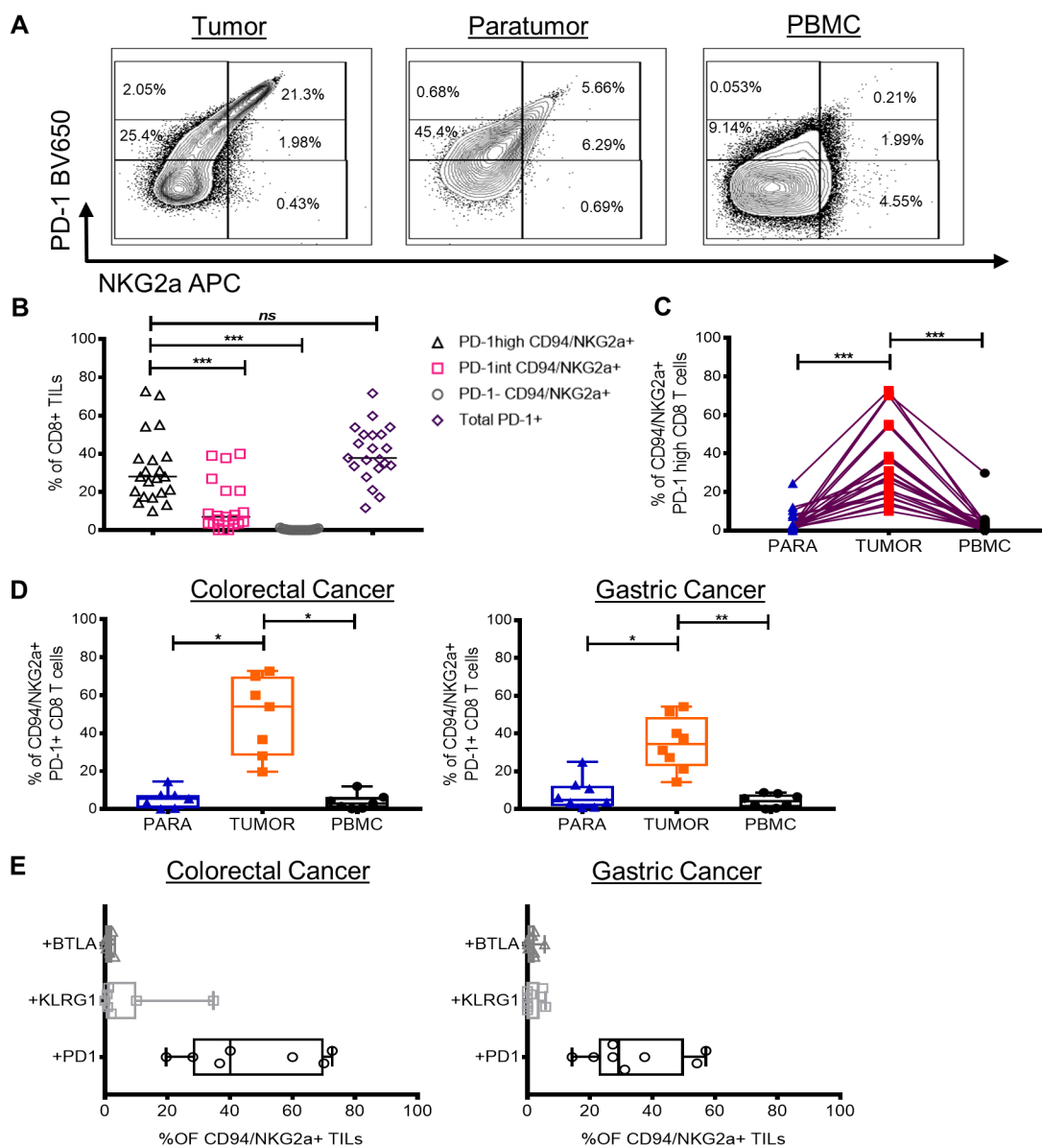


Figure 4

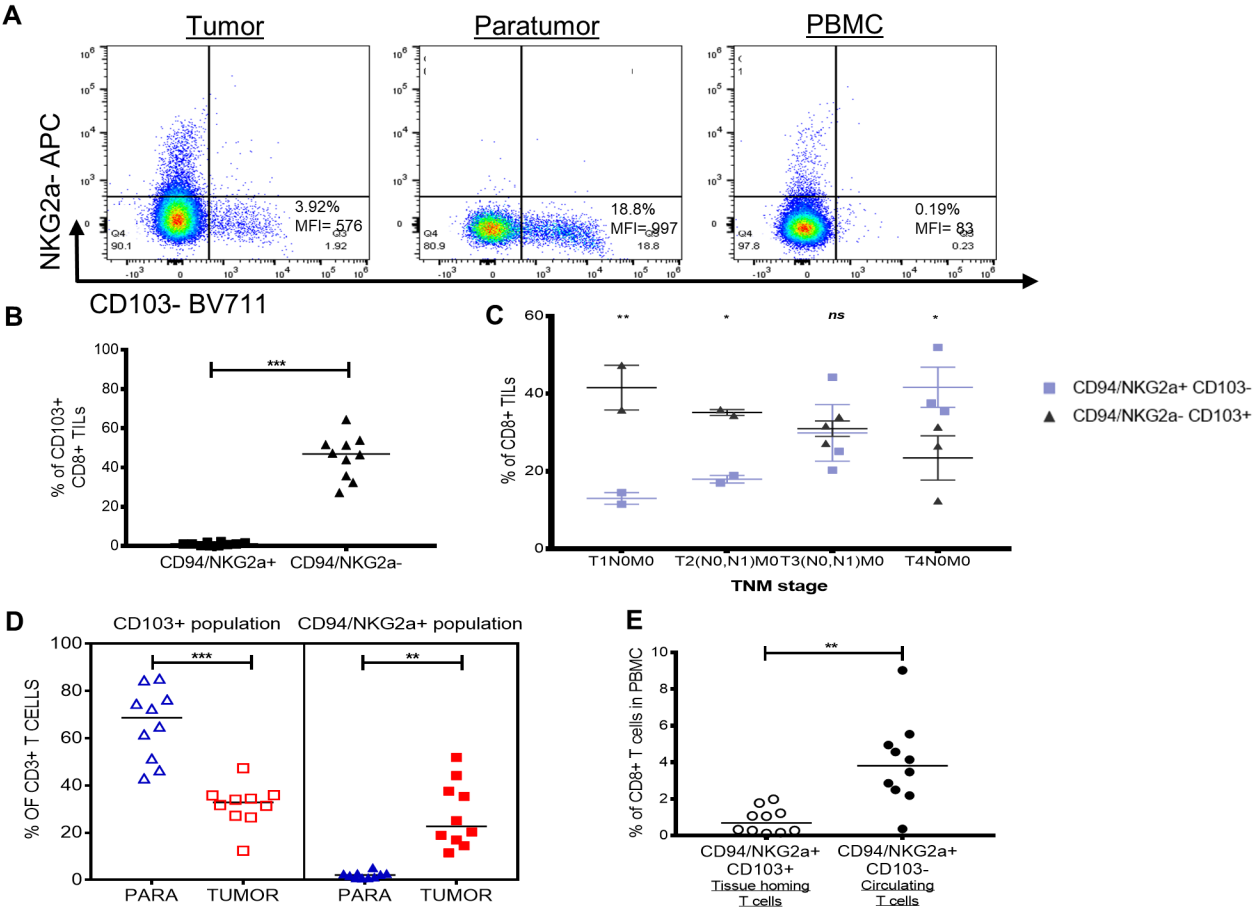


Figure 5

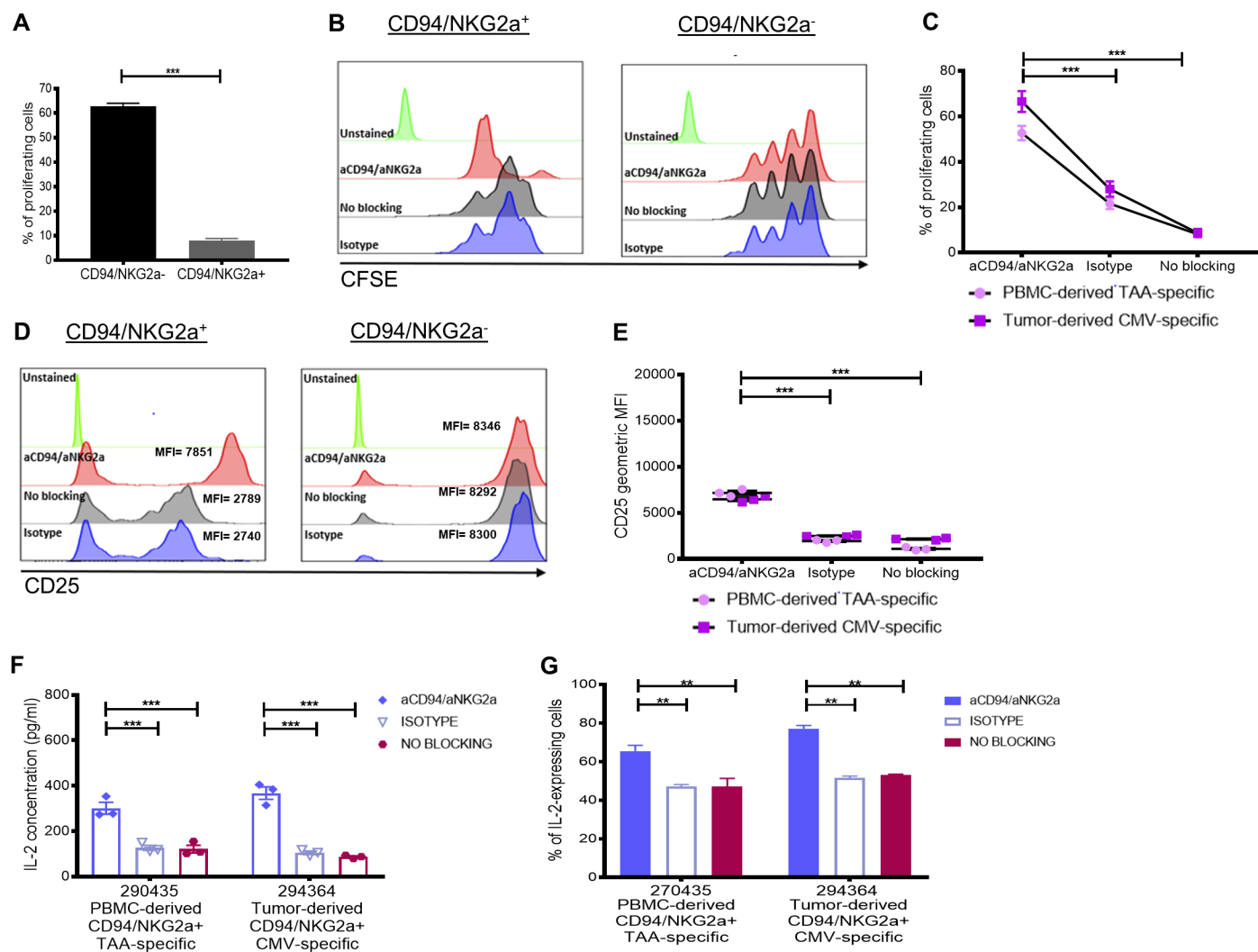


Figure 6

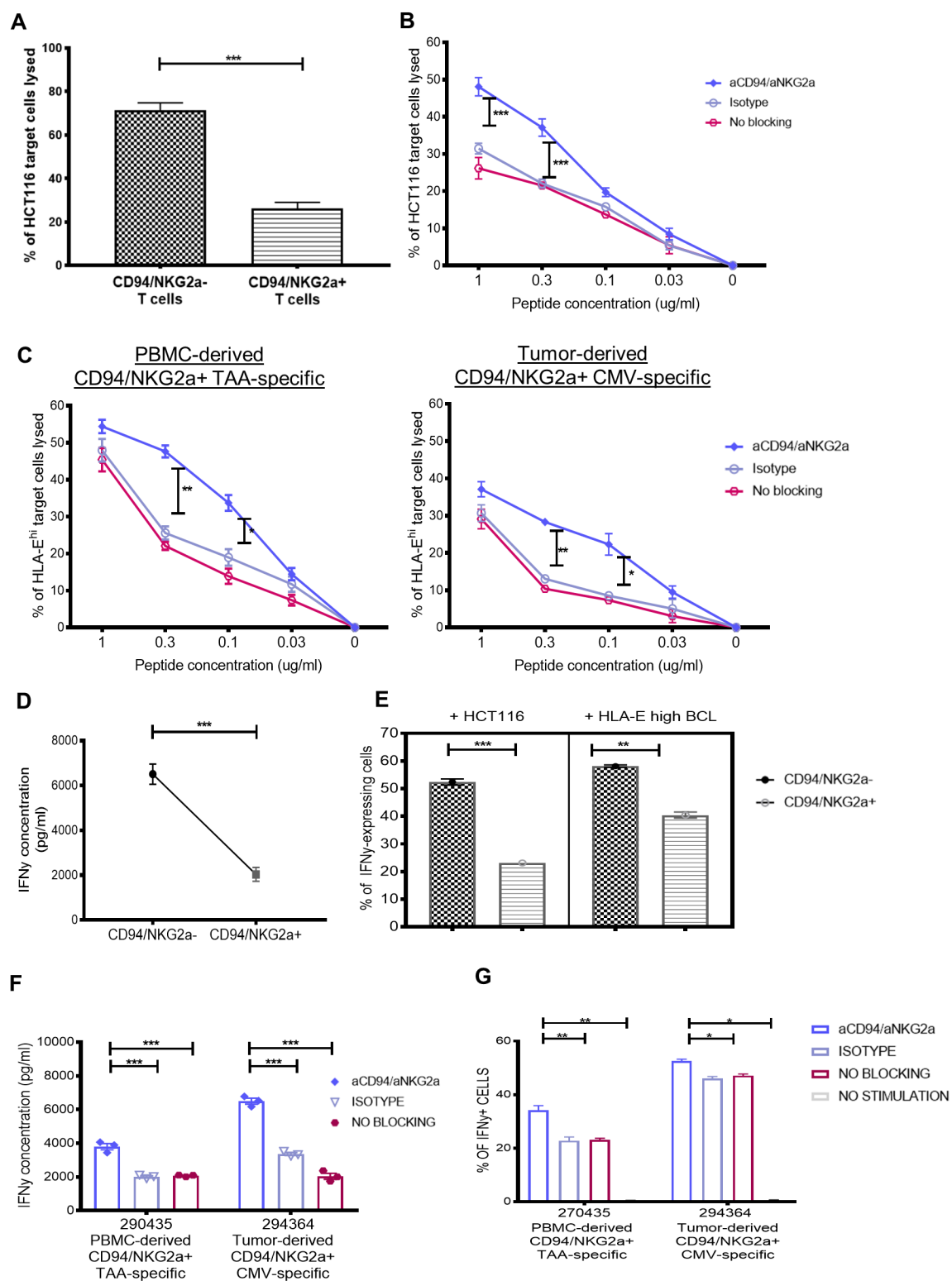


Figure 7

